Received: 5 February 2021 | Revised: 7 August 2021 | Accepted: 18 November 2021

DOI: 10.1002/jcla.24158

RESEARCH ARTICLE

WILEY

Upregulation of CD3ζ and L-selectin in antigen-specific cytotoxic T lymphocytes by eliminating myeloid-derived suppressor cells with doxorubicin to improve killing efficacy of neuroblastoma cells in vitro

Weili Xu | **Suolin Li** | **Meng Li** | **Hui Zhou** | **Xiaofeng Yang**

Department of Pediatric Surgery, The Second Hospital of Hebei Medical University, Shijiazhuang, China

Correspondence
Weili Xu, Department of Pediatric Surgery, The Second Hospital of Hebei Medical University, 215 Heping West Road, Shijiazhuang City, Hebei Province 050000, China.
Email: drxu9916@163.com

Funding information
National Natural Science Foundation of China, Grant/Award Number: 81472503

Abstract

Background: Agglomeration of myeloid-derived suppressor cells (MDSCs) in tumors impedes immunotherapeutic effects. Doxorubicin (DOX) is currently the most specific drug used for the selective removal of MDSCs. Here, we study the feasibility and mechanism of eliminating MDSCs by DOX to improve antigen-specific cytotoxic T lymphocyte (CTL)-killing neuroblastoma (NB) cells *in vitro*.

Methods: CTL and MDSC were prepared; then, CTLs, NB cells, MDSCs, and DOX were mixed and cultivated in different collocation patterns and divided into different groups. The levels of cluster of differentiation 3ζ chain (CD3ζ) and L-selectin in CTL in different groups were detected. Thereafter, the killing rate of NB cells and secretion of interleukin-2 and interferon-γ were measured and compared.

Results: By real-time polymerase chain reaction (PCR) and Western blot test respectively, the proliferation and killing effect of CTLs on NB cells were all inhibited by MDSC through downregulating CD3ζ ($p = 0.002$; $p = 0.001$) and L-selectin ($p = 0.006$; $p < 0.001$). However, this inhibitory effect was reversed by DOX. Significant differences were observed in the levels of interleukin-2 ($p < 0.001$), interferon-γ ($p < 0.001$), and the killing rate ($p < 0.001$) among the groups, except between the CTL +SK-N-SH and CTL +SK-N-SH +DOX groups ($p > 0.05$).

Conclusions: Targeted elimination of MDSCs by DOX can improve Ag-specific CTL killing of NB cells *in vitro* by upregulating CD3ζ and L-selectin. This study provides a novel method to enhance the immunotherapeutic effects of NB.

KEYWORDS
cytotoxic T lymphocyte, doxorubicin, in vitro, myeloid-derived suppressor cell, neuroblastoma

1 | INTRODUCTION

Neuroblastoma (NB) is the most common pediatric neuroendocrine tumor with high malignancy and early metastasis.[1] The survival rate of children with high-risk NB is still less than 40%, although many therapeutic methods, including surgery, radiotherapy, chemotherapy, and stem cell transplantation, have been adopted.[1–4] Although immunotherapy has recently been started for children with solid tumors, many studies have shown that immunotherapy with NB can effectively remove tumor cells and reduce tumor recurrence and metastasis with higher specificity and less toxicity compared to traditional therapy.[5,6]

However, in the survival microenvironment of NB, many complicated immunosuppressive factors impede therapeutic effects, resulting in immune tolerance, including downregulation of HLA-I antigen and accumulation of various immunosuppressive cells, such as myeloid-derived suppressor cells (MDSCs), regulatory T cells, and tumor-associated macrophages.[7–9] Currently, new approaches targeting the tumor microenvironment hold promise for further improvements in survival and long-term quality of life.[10] Furthermore, Jales et al. found that high expression of disialoganglioside on the surface of NB resulted in increased MDSC agglomeration in the tumor microenvironment,[11] which triggered tumor immunosuppression and promoted the development and metastasis of tumors. Thus, for these factors, MDSC may be the main impediment to NB immunotherapy. Some studies have shown that MDSCs cause dissociation between T-cell receptor (TCR) and cluster of differentiation 3ζ (CD3ζ) molecules, disrupting TCR complexes on T cells, which results in Ag-specific $CD8^+$ T-cell tolerance in cancer.[12,13] MDSCs downregulate L-selectin levels in naive T cells, decreasing their ability to home to sites where they are activated.[14,15]

In recent years, the study of MDSCs as a regulatory target to improve the immune efficacy of tumors has gradually emerged.[16,17] Alizadeh et al. reported that doxorubicin (DOX) can be used as a potent immunomodulatory agent that selectively impairs MDSC-induced immunosuppression in breast cancer.[18] However, in neuroblastoma, the effective removal of MDSCs from the microenvironment to improve the effector cell killing effect on tumor cells has rarely been studied. Thus, in this study, the feasibility and mechanisms of eliminating MDSCs by DOX to enhance antigen-specific cytotoxic T lymphocyte (CTL) killing of NB cells were explored, in order to provide a new method to enhance the immune therapeutic effects of NB.

2 | MATERIALS AND METHODS

2.1 | Cell lines and animals

SK-N-SH cells, obtained from the Shanghai Cell Bank of the Chinese Academy of Medical Sciences, were maintained in DMEM (P-04–03590, Gibco) with 10% fetal calf serum (10082–147, Gibco) and cultivated at 37°C in a 5% CO_2 humidified incubator. Six-week-old female BALB/c mice, each weighing 18–20 g (SCXK Hebei 2008–1–003), were purchased from the Experimental Animal Center of Hebei Province (SPF grade, SYXK Hebei 2008–0026) and housed in a specific pathogen-free facility. Spirit, diet, and defecation were regularly observed and recorded. All experiments were conducted in accordance with the principles and procedures outlined in the guidelines of the Institutional Experimental Animal Review Committee.

2.2 | Separation and purification of MDSCs in vitro

BALB/c mice were sacrificed, and bone marrow cells were extracted and made into a single-cell suspension. After red blood cells had been cracked, the cell suspension was administrated by anti-Gr-1 monoclonal Ab (mAb) (85–11–5320–82, eBioscience), anti-CD11b mAb (85–12–0113–42, eBioscience), anti-CD80 mAb (85–12–0809–42, eBioscience), anti-F4/80 mAb (bs-7058R-FITC, Bioss), anti-CD11c mAb (85–12–0116–42, eBioscience), and anti-MHC-II mAb (85–11–5320–82, eBioscience). Differentiation of MDSCs and the proportion of $Gr\text{-}1^+CD11b^+$MDSCs were analyzed by flow cytometry. IgG FITC, a homotypic control antibody, was used to set the gate strategy.

Bone marrow cells were suspended in PBS, and MDSCs were separated by Percoll density gradient centrifugation (P8370, Solarbio). Subsequently, cell suspensions were collected and separated using CD11b magnetic beads (130–049–601, Miltenyi, Germany), and the purity of $Gr\text{-}1^+CD11b^+$ MDSCs was verified by flow cytometry.

2.3 | Preparation of NB antigen-specific cytotoxic T lymphocyte

2.3.1 | Extraction and cultivation of BALB/c mice bone marrow-derived dendritic cells

BALB/c mice were sacrificed, and bone marrow cells were extracted and made into a single-cell suspension. After the red blood cells had lysed, the cell suspension was cultivated at a concentration of 10^6/ml cells/mL. Thereafter, rmGM-CSF (20 ng/ml) (300–03, PeproTech) and rmIL-4 (20 ng/ml) (200–04, PeproTech) were added. On the sixth day, the morphology of dendritic cells (DCs) was observed by phase-contrast microscopy, and the expression rates of CD11c, CD86, and MHC-II were detected by flow cytometry. A homotypic IgG FITC antibody was used to set the gate strategy.

2.3.2 | Tumor antigen loading DC

SK-N-SH cells in the logarithmic phase were resuspended and adjusted to a concentration of 2×10^7/ml cells/ml. Cells were quickly frozen to −80 °C and then rewarmed in 37°C water. After four cycles, the cell suspension was centrifuged at 11180 × *g* for 15 min, and the supernatant was collected and cryopreserved at −80 °C. The lysate equivalent

TABLE 1 Real-Time PCR information

Gene	Primer sequence	Amplification, bp
CD3ζ	Forward-ATCATCACAGCCCTGTACC Reverse-TCATATTCCTCTCTTCGCC	119
L-Selectin	Forward-CAACCCCCTCTTCATTCC Reverse-TGCCTTTTTTTAACCGCC	92
β-Actin	Forward-GGCACCACACCTTCTAC Reverse-CTGGGTCATCTTTTCAC	107

Abbreviations: CD3ζ, cluster of differentiation 3 ζ chain; PCR, polymerase chain reaction.

of 2×10^6 tumor cells was added per milliliter of DCs and cultivated for 6 days. Four hours later, rmTNF-α (300-01A, PeproTech) was added to the cell suspension and cultivated for 7th day. Subsequently, the suspension cells were collected and tumor antigen-loaded DCs were defined. The cell morphology of DCs was observed using a phase contrast microscope. Meanwhile, the expression rates of CD11c, CD86, and MHC-II were detected by flow cytometry.

2.3.3 | Extraction, identification, and cultivation of $CD3^+$ T cells

$CD3^+$ T cells were extracted from mouse spleen lymphocyte suspension using mouse $CD3^+$ T-cell magnetic beads (130–050–101, Miltenyi). Magnetic-activated cell sorting (MACS) can be repeated several times, and approximately 3×10^6 T lymphocytes can be extracted from each mouse spleen. Purified lymphocytes were collected, and the purity of $CD3^+$ T cells was determined. The concentration of cells was adjusted to 5×10^6/ml and cultivated for 2 days in medium containing rmIL-2 (20 ng/ml) (200–02, PeproTech). Cell morphology was observed under a phase-contrast microscope (CKX41-A32PH, Olympus), and cell viability was tested using Trypan blue (T8070, Solarbio).

2.3.4 | Preparation of NB-specific CTL and cytokine release test

After $CD3^+$ T cells were cultivated for 2 days, DCs loaded with tumor antigen and DCs non-loaded tumor antigen were added, according to the proportion of DC:T = 1:20. Thereafter, the morphology of the T cells was observed under an inverted microscope. After T cells had been activated for 72 h, the supernatants in each group were retained and concentrations of interleukin-2 (IL-2) and interferon-γ (IFN-γ) were calculated according to the absorbance value and the standard curve measured by the enzyme standard instrument. IL-2 and IFN-γ levels in the supernatants of the different groups were then compared.

2.4 | MDSC inhibiting proliferation of NB antigen-specific CTL

The activated CTLs were stained with 5,6-carboxyfluorescein diacetate succinimidyl ester (CFSE) (21888-25MG-F, Sigma) (concentration of CFSE was 5 μmol/L 19,20) and divided into two groups. In one group, CTLs were mixed with $Gr\text{-}1^+CD11b^+$ MDSCs (4:1), separated by MACS, and stimulated by CD3/CD28 antibody (85–11–0036-42/85-12–0289–42, eBioscience). Meanwhile, in another group, everything was the same, except for the absence of MDSC. A parallel control group was set up for each group using the same method as the experimental group. After cultivation for 4 days, the mixed cell system was observed by fluorescence microscopy (CX41-32RFL, Olympus, Japan) and cell proliferation was detected by flow cytometry. A homotypic IgG FITC antibody was used to set the gate strategy.

2.5 | Detection of CD3ζ and L-selectin in CTL by real-time polymerase chain reaction and western blot

CTL, CTL + DOX(2 μmol/L), CTL + MDSC(1:4), and CTL + MDSC(1:4) + DOX(2 μmol/L) were incubated. The contents of CD3ζ and L-selectin in CTLs of the different groups were assessed and compared by real-time polymerase chain reaction (PCR). Total RNA was isolated from the samples using an ultra-pure RNA extraction kit, according to the manufacturer's guidelines (CW0597S, Cwbio, Co. Ltd.). For reverse transcription, 1 μg of RNA was used to synthesize single-stranded cDNA (HiFi-MMLV cDNA first-strand synthesis kit; CW0744M, Cwbio, Co. Ltd.), according to the manufacturer's guidelines. Real-time PCR was performed using a fluorescence quantitative PCR amplifier (LightCycler 480 II, Roche), as described previously. Triplicate reactions were set up for each gene in a 96-well plate. The reaction information is summarized in Table 1. Amplification was performed using the following program: initial denaturation at 95°C for 15 min, followed by 40 cycles of 95°C for 10 s, 58°C for 30 s, and 72°C for 30 s. The experimental data were expressed as relative expression using the $2^{-\Delta\Delta Ct}$ equation, as described previously.[21]

Proteins were extracted with RIPA lysis buffer (89901, Thermo Fisher) and quantified using the BCA Protein Assay Kit (23225, Thermo Fisher). The samples were separated by 12% SDS-PAGE (A1054, Solarbio), transferred to a PVDF membrane (ISEQ00010, Millipore), and blocked with 5% BSA (SW3015, Solarbio). Primary antibodies against each protein were added and incubated at 4°C overnight. Subsequently, the secondary antibodies were added and incubated for 4 h at 20°C. After washing the membrane, chemiluminescence was detected on X-ray film using FluorChem®HD2 (Alpha Innotech), with GAPDH as the internal reference.

2.6 | MDSCs regulating the killing effect of NB antigen-specific CTL in vitro

CTL, DOX(2 μmol/L), CTL + DOX(2 μmol/L), CTL + MDSC (1:4), and CTL + MDSC(1:4) + DOX(2 μmol/L) were mixed with SK-N-SH cells and incubated (CTL:SK-N-SH = 20:1). At the same time, the blank control, target cell, and effector cell groups were set up. CCK-8 (C0038, Biyuntian) was added to the cell system (20 μl/hole) after incubation, and the absorbance value (A value) was detected at 450 nm wavelength using an enzyme standard instrument. The cytotoxic activities of the effector cells were evaluated based on the killing rate. The killing rate of effector cells was calculated as follows: kill rate (%) = [A value of target cell group - (A value of experimental group - A value of effector cells group)]/A value of target cell group ×100%. Ten visual fields were observed in each group, and the killing rates of CTLs to SK-N-SH cells between the groups were evaluated and compared. The secretion levels of IL-2 and IFN-γ in the supernatant between the groups were detected and compared using enzyme-linked immunosorbent assay (ELISA).

2.7 | Statistical analysis

All data were analyzed using the SAS software (ver. 8 for Windows; SAS Institute Inc.). The Wilcoxon two-sample test and repeated-measures analysis of variance were used to analyze the results. Statistical significance was set at $p < 0.05$.

3 | RESULTS

3.1 | Extraction and identification of MDSCs, preparation of NB Ag-specific CTL, and cytokine release test

Percoll density gradient centrifugation showed that the rates of Gr-1$^+$ MDSCs, CD11b$^+$ MDSCs, CD11c$^+$ MDSCs, CD80$^+$ MDSCs, F4/80$^+$ MDSCs, and MHC-II$^+$ MDSCs were 70.4%, 3.5%, 4.8%, 1.2%, 0.3%, and 2.1%, respectively (Figure 1A), and the rate of Gr-1$^+$CD11b$^+$ MDSCs was 22.6% (Figure 1B). Furthermore, MDSC suspension was sorted by CD11b magnetic beads, and purification of Gr-1$^+$CD11b$^+$ MDSCs was shown to be 84.6% by flow cytometry (Figure 1C). By flow cytometry, the expression rates of CD11c, CD86, and MHC-II on antigen-loaded DCs were 10.9%, 3.8%, and 27.9%, respectively, which suggested a weaker antigen-presenting ability (Figure 1D). Most DCs showed adherent growth with different sizes, star or spindle shapes, and stretching tubers. At the 7th day, DCs were activated by the tumor antigen. DCs in the half-adherent state increased clearly, with radial spikes and larger shapes. The expression rates of CD11c, CD86, and MHC-II were 74.8%, 50.3%, and 49.8%, respectively, indicating the presence of mature DCs with efficient antigen presentation ability (Figure 1E). CD3$^+$ T cells, extracted from spleen lymphocytes by MACS, reached 87.3% by flow cytometry. The living cell rate was 96.38% using the Trypan blue test. After 3 to 4 days of cultivation with antigen-loaded DCs, antigen-specific CD3$^+$ T cells were prepared and gathered into many small colonies. The levels of interleukin-2 (IL-2) (1.092 ± 0.010 ng/l) and interferon-γ (0.855 ± 0.038 ng/l) in the supernatant of antigen-loaded CD3$^+$ T cells were significantly higher than those of IL-2 (0.962 ± 0.007 ng/l) and IFN-γ (0.765 ± 0.010 ng/l) in the supernatant of CD3$^+$ T cells without antigen loading ($p < 0.05$).

3.2 | MDSC inhibiting proliferation of CTL

Under fluorescence microscopy, the number of CTLs was the same in the two groups before cultivation (Figure 2A). However, after cultivation for 4 days, the cells proliferated, but staining intensity weakened in the CTL group. In contrast, in the CTL +MDSC group, the cell number scarcely increased and staining intensity remained strong (Figure 2B).

Flow cytometry analysis revealed consistent results. In the CTL +MDSC group, CTLs with strong fluorescence (87.6%) were much higher than those with weak fluorescence. However, the strong fluorescence CTLs (44.1%) were less abundant than the weakly fluorescent CTLs in the CTL group (Figure 2C).

3.3 | Downregulation of CD3ζ and L-selectin in CTL by MDSC

The levels of CD3ζ and L-selectin in CTL were detected and compared by real-time PCR (Figure 3A) and Western blot analysis (Figure 3B). In the real-time PCR test, significant differences in CD3ζ ($F = 71.981$, $p < 0.001$) and L-selectin ($F = 80.712$, $p < 0.001$) were observed among the groups, except for between the CTL and CTL+DOX groups. Western blot analysis showed similar results. Significant differences in CD3ζ ($F = 33.098$, $p < 0.001$) and L-selectin ($F = 53.749$, $p < 0.001$) were also observed among the groups, except for the CTL and CTL+DOX groups.

3.4 | DOX inhibits MDSC and then enhances the killing effect of CTL in vitro

Under an inverted microscope, the killing process of CTLs to SK-N-SH cells was clearly observed in each group. From Day 1 to Day 10, we found that in the CTL +SK-N-SH +MDSC groups, SK-N-SH cells were still scattered, with a relatively regular outline. However, in the CTL +SK-N-SH, CTL +SK-N-SH +DOX, and CTL +SK-N-SH +MDSC + DOX groups, nearly all the SK-N-SH cells exhibited apoptosis or necrosis, and CTLs also decreased significantly. During the whole period, in the SK-N-SH and SK-N-SH +DOX groups, tumor cells proliferated continuously and

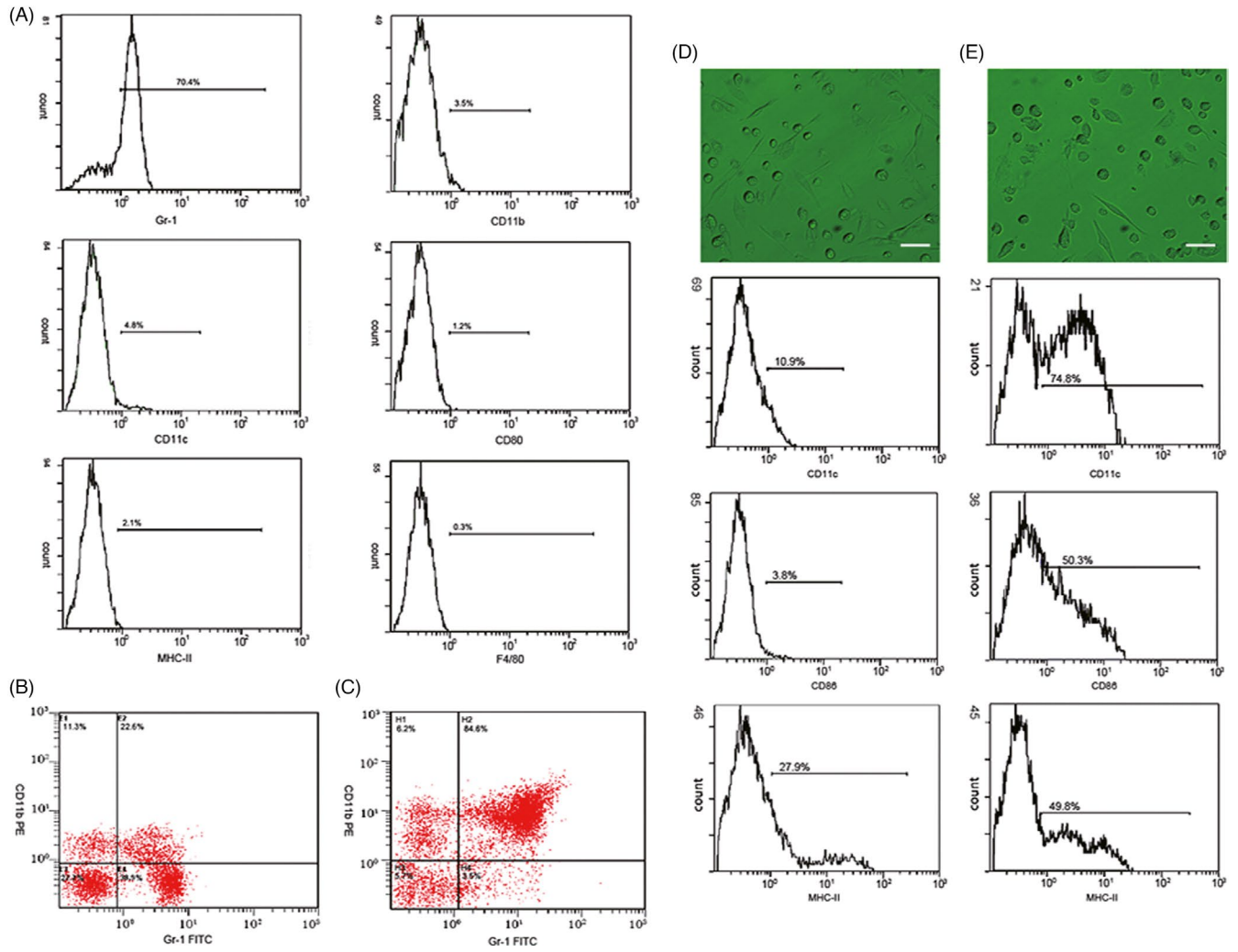

FIGURE 1 Extraction, identification, and purification of myeloid-derived suppressor cell and cultivation of dendritic cell. (A) Cells were extracted from the bone marrow of BALB/c mice and stained by monoclonal antibodies. Under flow cytometry, the expressive rate of Gr-1$^+$MDSC, CD11b$^+$MDSC, CD11c$^+$MDSC, CD80$^+$MDSC, F4/80$^+$MDSC, and MHC-II$^+$MDSC were 70.4%, 3.5%, 4.8%, 1.2%, 0.3%, 2.1% respectively. (B) The expressive rate of Gr-1$^+$CD11b$^+$MDSC was 22.6%. (C) After MACS by CD11b magnetic bead, purification of Gr-1$^+$CD11b$^+$MDSC reached 84.6%. (D) Most non-antigen-loaded dendritic cells grew adherently, with different sizes, star or spindle shape, and stretching tubers, but some of the cells seemed to have adopted a half-adherent state with rough surface. The expressive rates of CD11c, CD86, and MHC-II on DCs were 10.9%, 3.8%, and 27.9%, respectively, by flow cytometry. (E) On the 7th day, DCs were stimulated and activated by tumor antigens. DCs in the half-adherent state increased obviously with radial spikes and bigger shape. The expressive rates of CD11c, CD86, and MHC-II were 74.8%, 50.3%, and 49.8%, respectively, by flow cytometry. IgG FITC, a homotypic control antibody, was used to set the gate strategy. *Scale bar* = 100 μmol/liter. MDSC, myeloid-derived suppressor cell; MACS, magnetic-activated cell sorting; DC, dendritic cell; CD, cluster of differentiation

remained active (Figure 4A). Thus, these results proved that the toxicity of low-dose DOX to the NB cells alone was not serious, but that doxorubicin inhibited MDSCs and enhanced the killing effect of CTL on SK-N-SH cells. The killing rates were determined based on the results obtained on Day 10. There was a significant difference in the killing rate between the groups ($F = 36.494$, $p < 0.001$), except between the CTL +SK-N-SH and CTL +SK-N-SH +DOX groups ($p = 0.217$) (Figure 4B). Levels of IL-2 and IFN-γ in the supernatant were detected by ELISA. The results of repeated measurement analysis of variance showed that there were significant differences in the secretion levels of IL-2 ($F = 188.589$, $p < 0.001$) and IFN-γ ($F = 631.433$, $p < 0.001$) among the groups, except for the CTL +SK-N-SH and CTL +SK-N-SH +DOX groups (Figure 4C and Figure 4D).

4 | DISCUSSION

At present, the most effective method of immunotherapy for NB is the adoptive transfer of chimeric GD2 antigen receptors CTL.[22,23] However, some phase III clinical trials have found that some children with high-risk NB who underwent adoptive cell transfer immunotherapy of chimeric GD2 antigen receptor CTLs still showed recurrence and metastasis, although the survival rates improved.

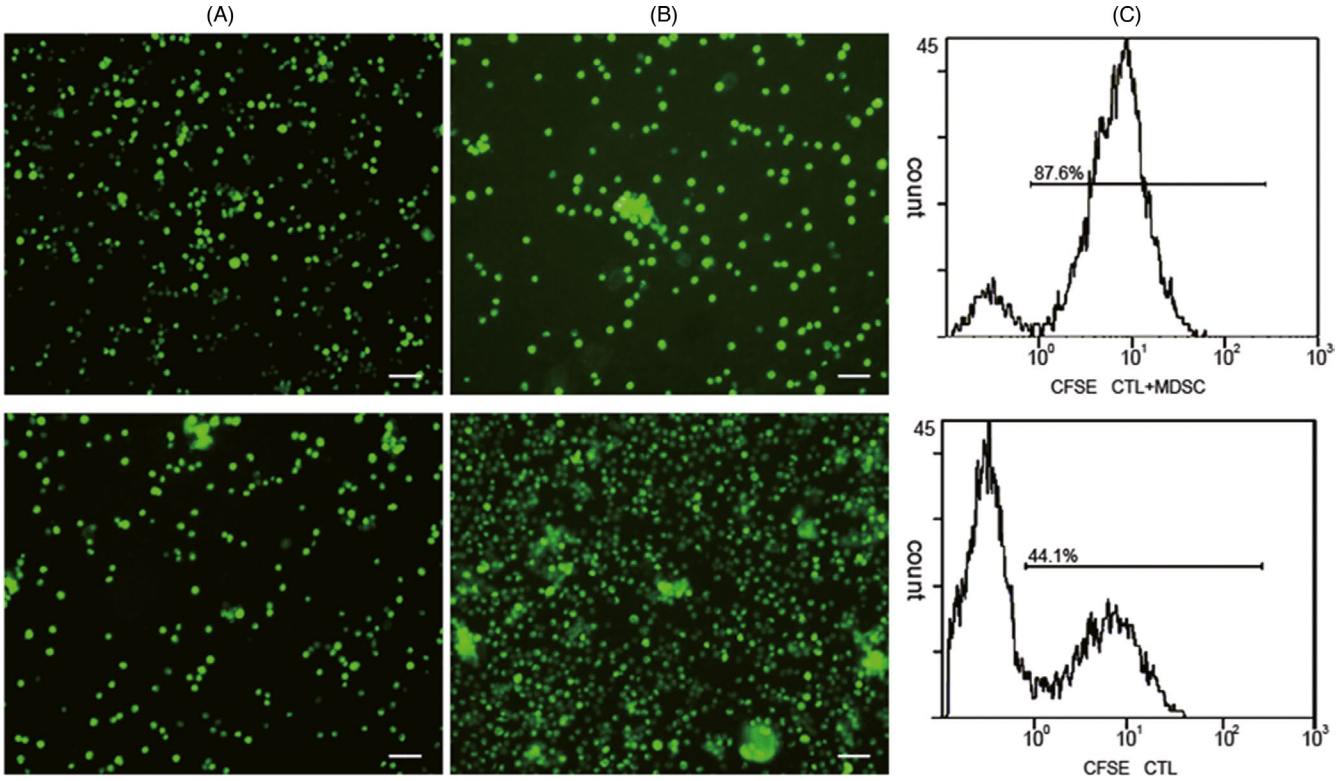

FIGURE 2 Myeloid-derived suppressor cells inhibit the proliferation of neuroblastoma antigen-specific cytotoxic T lymphocyte. Neuroblastoma antigen-specific CTLs in the two groups were stained by CFSE. (A) Under fluorescence microscopy, the same number of CTLs was seen in the CTL and CTL +MDSC groups before cultivation (200 times magnification). (B) After cultivation for 4 days, cell proliferation progressed, but fluorescent intensity weakened in the CTL group. However, in the CTL + MDSC group, the cell fluorescent intensity remained strong, while the cell number scarcely increased (200 times magnification). (C) Flow cytometry showed results consistent with those obtained by microscopy. After cultivation, in the CTL + MDSC group, the rate of CTLs with strong fluorescence was 87.6%. However, only 44.1% of CTLs with strong fluorescence were found in the CTL group. IgG FITC, a homotypic control antibody, was used to set the gate strategy. *Scale bar* = 100 μmol/liter. CTL, cytotoxic T lymphocyte; CFSE, 5,6-carboxyfluorescein diacetate succinimidyl ester; MDSC, myeloid-derived suppressor cell

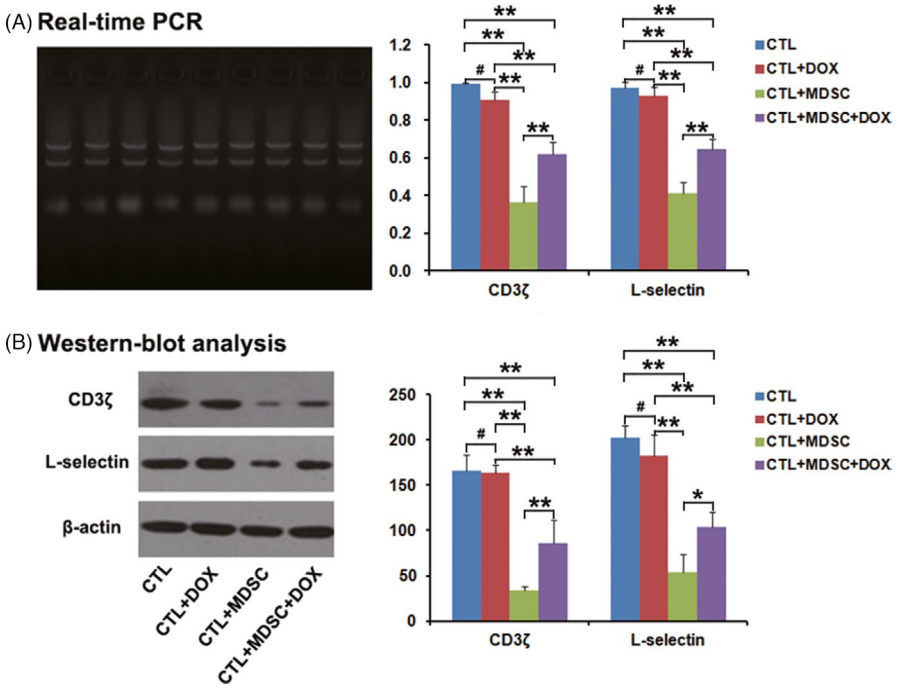

FIGURE 3 Expressions of cluster of differentiation 3ζ and L-selectin in antigen-specific cytotoxic T lymphocytes. The levels of CD3ζ and L-selectin in CTL were detected and compared by real-time PCR and Western blot analysis, respectively. (A) In real-time PCR test, significant difference of CD3ζ ($p < 0.001$) and L-selectin ($p < 0.001$) were found between the groups, except for the CTL and CTL +DOX groups ($p = 0.160$). (B) Western blot analysis showed a significant difference in CD3ζ ($p < 0.001$) and L-selectin ($p < 0.001$) among the groups, except for the CTL and CTL +DOX groups ($p = 0.054$). $^{*}p < 0.05$; $^{**}p < 0.01$; $^{\#}p > 0.05$. CD3ζ, cluster of differentiation 3 ζ chain; PCR, polymerase chain reaction; CTL, cytotoxic T lymphocyte; DOX, doxorubicin

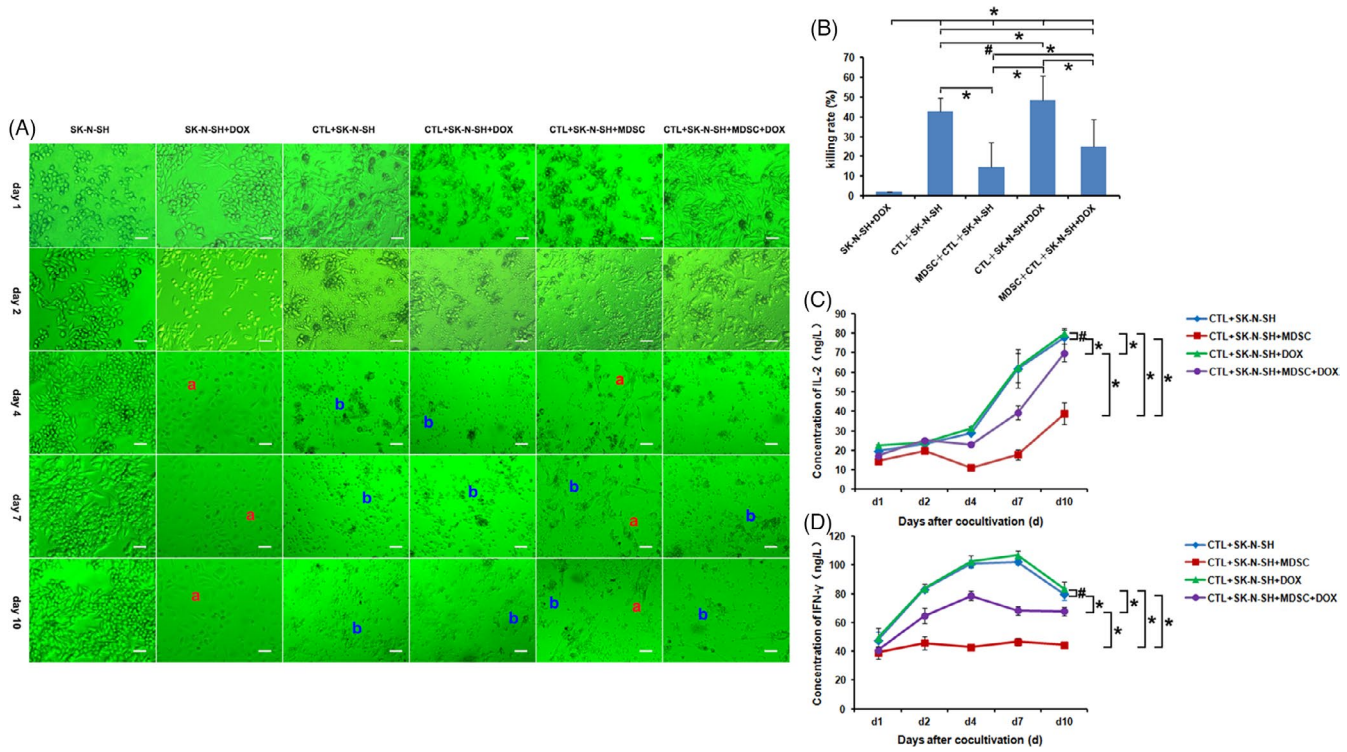

FIGURE 4 Eliminating myeloid-derived suppressor cell with doxorubicin to improve killing efficacy of cytotoxic T lymphocyte. (A) On the 1st day, CTLs or DOX was mixed with SK-N-SH cells, and no difference was seen between the groups. On the 2nd day, in the CTL + SK-N-SH group, CTL + SK-N-SH + DOX group, and CTL + SK-N-SH +MDSC + DOX group, CTLs and SK-N-SH cells gathered and began to interact; however, CTLs and SK-N-SH cells scattered in view in CTL + SK-N-SH +MDSC group. On the 4th day, in CTL + SK-N-SH + MDSC group, CTLs and SK-N-SH cells all proliferated. However, in the other three groups, CTLs proliferated but SK-N-SH cells began to deform. On the 7th day, in CTL + SK-N-SH group, CTL + SK-N-SH + DOX group, and CTL + SK-N-SH + MDSC + DOX group, SK-N-SH cells further deformed and lost their cellular shape, while the number of CTLs began to decrease. However, SK-N-SH cells kept a regular shape in the CTL + SK-N-SH + MDSC group. On the 10^{th} day, in the CTL + SK-N-SH + MDSC groups, SK-N-SH cells still scattered in view with regular outline. However, in the other three groups, nearly all of the SK-N-SH cells appeared to be apoptotic or necrotic, while the number of CTLs also decreased significantly. During the whole period, in SK-N-SH group and SK-N-SH +DOX group, the tumor cells kept their active state. The red "a" denotes SK-N-SH cells with a regular outline, while the blue "b" denotes apoptotic or necrotic cell fragments. B, A significant difference existed in the killing rate between the groups ($p < 0.001$), except for between the CTL +SK-N-SH group and the CTL + SK-N-SH +DOX group ($p = 0.217$). C and D, IL-2 and IFN-γ in the supernatant were detected by ELISA. By repeated measurement analysis of variance, there were significant differences in the levels of IL-2 ($p < 0.001$) and IFN-γ ($p < 0.001$) among the groups except CTL + SK-N-SH group and CTL +SK-N-SH +DOX group. $^{*}p < 0.05$; $^{\#}p > 0.05$. *Scale bar* = 100 μmol/liter. CTL, cytotoxic T lymphocyte; MDSC, myeloid-derived suppressor cell; DOX, doxorubicin; IL-2, interleukin-2; IFN-γ, interferon-γ

This suggests that this kind of passive immunotherapy needs to improve its curative effect by adjusting the immunosuppressive microenvironment.[6,24]

In the tumor microenvironment, accumulation of a variety of immunosuppressive cells, including MDSCs, is the main immunosuppressive factors and results in immune tolerance and disability of the immune system.[25,26] MDSCs are a group of innate immune cells that originate from myeloid cells which play a negative immune regulatory role in tumor progression.[27,28] MDSCs inhibit the body's natural immune and T-cell adaptive immune responses.[29,30] Therefore, MDSCs induce tumor immune tolerance and are thus the main impediment to immunotherapy.

The role of MDSCs in NB remains unclear, although the mechanism of MDSCs in other tumors has been extensively explored. In the present study, NB Ag-specific CTLs were stained with CFSE. The cytoplasm with fluorescent protein was evenly distributed to the next generation of cells, and the fluorescence intensity was reduced by half when cells proliferated continuously. Thus, the greater the generation of cell division, the weaker the cell fluorescence intensity. Therefore, the fluorescence intensity of CTL became weaker and the number of CTLs increased in CTLs cultivated without MDSC. In contrast, cell proliferation decreased and fluorescence intensity remained unchanged when CTLs were cultivated with MDSCs. The results show that MDSCs inhibit the proliferation of NB Ag-specific CTLs.

In further studies, the expression of CD3ζ and L-selectin in Ag-specific CTLs decreased significantly when CTLs were cultivated with MDSCs, but the expression of these two proteins increased again after DOX administration. As a chain of CD3 molecules, CD3ζ plays a key role in signal transmission inside and outside the cell.[12,13] The increased expressive activity of the ζ chain promotes TCR-identified intracellular immune signal transmission, which leads to activation of T

cells and production of cytokines, such as IL-2 and IFN-γ.[31] Moreover, L-selectin is an important molecule involved in the extravasation of lymphocytes from blood and lymphatic vessels and their homing to lymph nodes and tumors.[14,15] Therefore, the results indicate that DOX could effectively reverse the inhibitory role of MDSCs on CD3ζ and L-selectin in Ag-specific CTLs, which can promote the activation and migration of Ag-specific CTLs and effectively kill NB cells.

In recent years, some studies have pointed out that CTL produces cytotoxicity to target cells in two separate ways, namely the perforin and PCD pathways mediated by Fas antigen molecules.[32,33] Of these, the perforin pathway plays a significant role in antiviral, intracellular bacteria, tumor, and immune pathology.[33] During the course of perforin treatment, CTL killed the tumor, while the cytokines IL-2 and IFN-γ were released. The more obvious the killing effect, the higher the concentrations of the cytokine, and vice versa. In the present study, the killing rate of NB cells and the levels of IL-2 and IFN-γ in the supernatant decreased significantly when CTLs were cultivated with MDSC. However, the inhibitory role of MDSCs can be reversed by DOX administration.

In the present study, DOX reversed the inhibition of MDSCs and improved the killing effect of CTL, but the toxicity of low-dose DOX to the NB cells alone was not serious. Some studies have shown that DOX can selectively eliminate MDSCs, promote the activity of immune effector cells, and improve the therapeutic efficacy of adoptively transferred T lymphocytes.[34] Therefore, in this study, we demonstrated the underlying mechanism by targeting the inhibition of MDSC by DOX to enhance Ag-specific CTLs killing NB cells in vitro.

ACKNOWLEDGMENTS

This study was supported by the National Natural Science Foundation of China (No.81472503). We thank Huizhen GENG, Jie ZHANG, and Luping LI for their technical assistance and the development facility for their help in sorting the dendritic cells and myeloid-derived suppressor cells. We also thank Prof. Zhen-yun Mou (Department of Statistics Research Office, Hebei Medical University) for his help with statistical analysis. The authors declare no financial conflicts regarding this work.

CONFLICTS OF INTEREST

All authors declare no conflicts of interest.

AUTHOR CONTRIBUTIONS

All authors contributed to the conception and design of the study. Material preparation, data collection, and analysis were performed by Weili Xu, Suolin Li, Meng Li, Hui Zhou, and Xiaofeng Yang. The first draft of the manuscript was written by Weili Xu, and all authors commented on the previous versions of the manuscript. All authors read and approved the final manuscript.

DATA AVAILABILITY STATEMENT

All authors make sure that all data and materials support their published claims. The data that support the findings of this study are available from the corresponding author upon reasonable request.

ORCID

Weili Xu https://orcid.org/0000-0001-6234-2805

REFERENCES

1. Mahapatra S, Kishore B. Cancer, neuroblastoma. Challagundla. *Stat Pearls [Internet]*. Stat Pearls Publishing; 2020.
2. Ryan AL, Akinkuotu A, Pierro A, Morgenstern DA, Irwin MS. The role of surgery in high-risk neuroblastoma. *J Pediatr Hematol Oncol*. 2020;42:1-7.
3. Lau SCD, Unni MNM, Teh KH, et al. Autologous stem cell transplantation following high-dose chemotherapy in children with high-risk neuroblastoma: practicality in resource-limited countries. *Pediatr Blood Cancer*. 2020;67:e28176.
4. Zhao Q, Liu Y, Zhang Y, et al. Role and toxicity of radiation therapy in neuroblastoma patients: a literature review. *Crit Rev Oncol Hematol*. 2020;149:102924.
5. Szanto CL, Cornel AM, Vijver SV, Nierkens S. Monitoring immune responses in neuroblastoma patients during therapy. *Cancers (Basel)*. 2020;12:519.
6. Casey DL, Cheung NV. Immunotherapy of pediatric solid tumors: treatments at a crossroads, with an emphasis on antibodies. *Cancer Immunol Res*. 2020;8:161-166.
7. Zhong X, Zhang Y, Wang L, Zhang H, Liu H, Liu Y. Cellular components in tumor microenvironment of neuroblastoma and the prognostic value. *PeerJ*. 2019;7:e8017.
8. Parihar R, Rivas C, Huynh M, et al. NK cells expressing a chimeric activating receptor eliminate MDSCs and rescue impaired CAR-T cell activity against solid tumors. *Cancer Immunol Res*. 2019;7:363-375.
9. Komohara Y, Takeya M. CAFs and TAMs: maestros of the tumour microenvironment. *J Pathol*. 2017;241:313-315.
10. Matthay KK, Maris JM, Schleiermacher G, et al. Neuroblastoma. *Nat Rev Dis Primers*. 2016;2:16078.
11. Jales A, Falahati R, Mari E, et al. Ganglioside-exposed dendritic cells inhibit T-cell effector function by promoting regulatory cell activity. *Immunology*. 2011;132:134-143.
12. Tumino N, Turchi F, Meschi S, et al. In HIV-positive patients, myeloid-derived suppressor cells induce T-cell anergy by suppressing CD3ζ expression through ELF-1 inhibition. *AIDS*. 2015;29:2397-2407.
13. Dar AA, Patil RS, Pradhan TN, Chaukar DA, D'Cruz AK, Chiplunkar SV. Myeloid-derived suppressor cells impede T cell functionality and promote Th17 differentiation in oral squamous cell carcinoma. *Cancer Immunol Immunother*. 2020;69:1071-1086.
14. Ku AW, Muhitch JB, Powers CA, et al. Tumor-induced MDSC act via remote control to inhibit L-selectin-dependent adaptive immunity in lymph nodes. *eLife*. 2016;5:e17375.
15. Perfilyeva YV, Abdolla N, Ostapchuk YO, et al. Chronic inflammation contributes to tumor growth: possible role of L-selectin-expressing myeloid-derived suppressor cells (MDSCs). *Inflammation*. 2019;42:276-289.
16. Hou A, Hou K, Huang Q, Lei Y, Chen W. Targeting myeloid-derived suppressor cell, a promising strategy to overcome resistance to immune checkpoint inhibitors. *Front Immunol*. 2020;11:783.
17. Chaib M, Chauhan SC, Makowski L. Friend or foe? recent strategies to target myeloid cells in cancer. *Front Cell Dev Biol*. 2020;8:351.
18. Alizadeh D, Trad M, Hanke NT, et al. Doxorubicin eliminates myeloid-derived suppressor cells and enhances the efficacy of adoptive T-cell transfer in breast cancer. *Cancer Res*. 2014;74:104-118.
19. Xu W, Cai J, Li S, et al. Improving the in vivo persistence, distribution and function of cytotoxic T lymphocytes by inhibiting the tumor immunosuppressive microenvironment. *Scand J Immunol*. 2013;78:50-60.
20. Xu W-L, Li S-L, Wen M, et al. Tracking in vivo migration and distribution of antigen-specific cytotoxic T lymphocytes by

5,6-carboxyfluorescein diacetate succinimidyl ester staining during cancer immunotherapy. *Chin Med J (Engl)*. 2013;126:3019-3025.
21. Schmittgen TD, Livak KJ. Analyzing real-time PCR data by the comparative C(T) method. *Nat Protoc*. 2008;3:1101-1108.
22. Long AH, Highfill SL, Cui Y, et al. Reduction of MDSCs with all-trans retinoic acid improves CAR therapy efficacy for sarcomas. *Cancer Immunol Res*. 2016;4:869-880.
23. Titov A, Valiullina A, Zmievskaya E, et al. Advancing CAR T-cell therapy for solid tumors: lessons learned from lymphoma treatment. *Cancers (Basel)*. 2020;12:125.
24. McNerney KO, Karageorgos SA, Hogarty MD, Bassiri H. Enhancing neuroblastoma immunotherapies by engaging iNKT and NK cells. *Front Immunol*. 2020;11:873.
25. Osipov A, Saung MT, Zheng L, Murphy AG. Small molecule immunomodulation: the tumor microenvironment and overcoming immune escape. *J Immunother Cancer*. 2019;7:224.
26. Hinshaw DC, Shevde LA. The tumor microenvironment innately modulates cancer progression. *Cancer Res*. 2019;79:4557-4566.
27. Lim HX, Kim TS, Poh CL. Understanding the differentiation, expansion, recruitment and suppressive activities of myeloid-derived suppressor cells in cancers. *Int J Mol Sci*. 2020;21:3599.
28. Dysthe M, Parihar R. Myeloid-derived suppressor cells in the tumor microenvironment. *Adv Exp Med Biol*. 2020;1224:117-140.
29. Gabrilovich DI. Myeloid-derived suppressor cells. *Cancer Immunol Res*. 2017;5:3-8.
30. Chen J, Ye Y, Liu P, et al. Suppression of T cells by myeloid-derived suppressor cells in cancer. *Hum Immunol*. 2017;78:113-119.
31. Weiss A, Littman DR. Signal transduction by lymphocyte antigen receptors. *Cell*. 1994;76:263-274.
32. Hassin D, Garber OG, Meiraz A, Schiffenbauer YS, Berke G. Cytotoxic T lymphocyte perforin and Fas ligand working in concert even when Fas ligand lytic action is still not detectable. *Immunology*. 2011;133:190-196.
33. Martínez-Lostao L, Anel A, Pardo J. How do cytotoxic lymphocytes kill cancer cells? *Clin Cancer Res*. 2015;21:5047-5056.
34. Hsu FT, Chen TC, Chuang HY, Chang YF, Hwang JJ. Enhancement of adoptive T cell transfer with single low dose pretreatment of doxorubicin or paclitaxel in mice. *Oncotarget*. 2015;6:44134-44150.

How to cite this article: Xu W, Li S, Li M, Zhou H, Yang X. Upregulation of CD3ζ and L-selectin in antigen-specific cytotoxic T lymphocytes by eliminating myeloid-derived suppressor cells with doxorubicin to improve killing efficacy of neuroblastoma cells in vitro. *J Clin Lab Anal*. 2022;36:e24158. doi:10.1002/jcla.24158